Zn-Porphyrin-Sensitized Nanocrystalline TiO_2 Heterojunction Photovoltaic Cells

Lukas Schmidt-Mende,[a] Wayne M. Campbell,[b] Qing Wang,[a] Kenneth W. Jolley,[b] David L. Officer,*[b] Md. K. Nazeeruddin,*[a] and Michael Grätzel*[a]

During the last 10 years, with the development of nanocrystalline films of very high surface area, the photosensitization of wide-bandgap semiconductors, such as TiO_2, by adsorbed dyes has become more realistic for solar-cell applications.[1–6] In a porous film consisting of nanometer-sized TiO_2 particles, the effective surface area can be enhanced 1000-fold, thus making light absorption efficient even though there is only a monolayer of dye on each nanoparticle.[7] Using ruthenium sensitizers and a nitrile-based electrolyte, the efficiency of nanocrystalline TiO_2 solar cells has reached more than 11% at AM 1.5 sunlight.[8] However, the main long-term limitation of these dye-sensitized solar cells is the use of liquid electrolytes. A solution to this problem is the replacement of the liquid electrolyte by a solid hole-conducting electrolyte.

For this reason, gel-based electrolytes,[9] polymers,[10] and p-type semiconductors have been extensively studied.[5, 11] Bach et al.[12] have demonstrated that the liquid electrolyte can be replaced by an amorphous organic hole-transport material 2,2′,7,7′-tetrakis(*N*,*N*-di-*p*-methoxyphenylamine)-9,9′-spirobifluorene (spiro-MeOTAD) creating a solid p-type semiconductor/TiO_2 heterojunction. This hole-conducting material allows the regeneration of the sensitizers after electron injection due to its efficient hole-transport properties. However, the overall cell conversion efficiency using the ruthenium dye [Ru(H_2dcbpy)$_2$($NCS)_2$] is significantly lower than the value of 11% observed for the corresponding liquid-junction cell.[13] The low efficiency may be due to the lack of intimate contact between the hydrophilic sensitizer and the hydrophobic hole conductor. Another possibility is that there is an insufficient light absorbance resulting from the fact that the thickness of the nanocrystalline TiO_2 film on the electrode is much less than that used in the liquid-junction cell.

It has been shown for TiO_2-bound tetrakis(carboxyphenyl)-porphyrins that the efficiency of electron injection into the TiO_2 conduction band and the kinetics of electron injection and recombination are indistinguishable from those of rutheni-

[a] *L. Schmidt-Mende, Q. Wang, Dr. M. K. Nazeeruddin, Prof. M. Grätzel*
Laboratory for Photonics and Interfaces
Institute of Chemical Sciences and Engineering
Swiss Federal Institute of Technology, 1015 Lausanne (Switzerland)
Fax: (+41) 21-693-6100
E-mail: mdkhaja.nazeeruddin@epfl.ch
michael.graetzel@epfl.ch

[b] *W. M. Campbell, K. W. Jolley, D. L. Officer*
Nanomaterials Research Centre and the MacDiarmid Institute
for Advanced Materials and Nanotechnology, Massey University
Private Bag 11222, Palmerston North 5301 (New Zealand)
Fax: (+64) 6-350-5612
E-mail: d.officer@massey.ac.nz

um polypyridyl sensitizers,[14] although liquid-junction cells incorporating these porphyrins have demonstrated only moderate cell efficiencies.[15] Recently, however, we reported a significant increase in cell efficiency using porphyrin sensitizers with fully conjugated carboxylate anchoring groups.[16] Given the potential to easily vary the hydrophobicity of the porphyrin sensitizer through phenyl-ring alkylation, and the possibility of increased TiO_2 surface coverage through close-packing of the dyes, these sensitizers appeared to be attractive possibilities for incorporation into photovoltaic heterojunctions.

Here, we report the application of green porphyrins cyano-3-(2′-(5′,10′,15′,20′-tetraphenylporphyrinato zinc(II))yl)acrylic acid **Zn-1** and 2-carboxy-5-(2′-(5′,10′,15′,20′-tetra(3″,5″-dimethylphenyl)porphyrinato zinc(II))yl)-penta-2,4-dienoic acid **Zn-2** as light harvesters in heterojunction devices, and the photovoltaic properties of the devices.

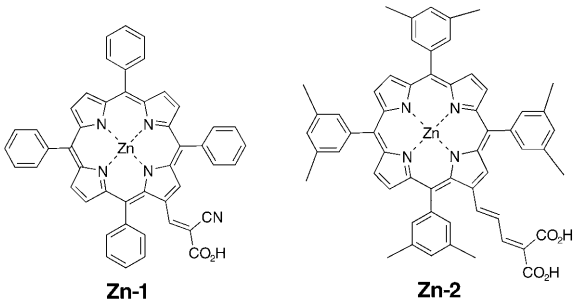

Figure 1. Chemical structures of **Zn-1** and **Zn-2**.

Figure 1 shows the structures of the two sensitizers, **Zn-1**, which has been reported previously,[17] and **Zn-2**, whose synthesis is described here (Scheme 1). Wittig reaction of tetraxylylporphyrin aldehyde **3**[18] with the phosphorane, ethyl (triphenylphosphoranylidene)-acetate, resulted in a *cis*/*trans* (≈42% *cis*) mixture of the vinyl ester. Isomerization of this mixture to the all-*trans* ester **4** was efficiently achieved with iodine. Oxidation of the alcohol **5**, produced from the DIBAL-H reduction of this ester **4**, with MnO_2 gave an excellent yield of the allylaldehyde **6**. A quantitative yield of the extended malonic-acid derivative **Zn-2** was obtained by malonic-acid condensation with aldehyde **6**, followed by metallation of the resulting product with zinc(II) acetate. The analytical and spectroscopic data for **Zn-2** are fully consistent with the structures. The introduction of the malonic-acid group into **Zn-2** results from our recent work, which shows that this group is a better anchoring group than the cyanoacrylic acid group.[19]

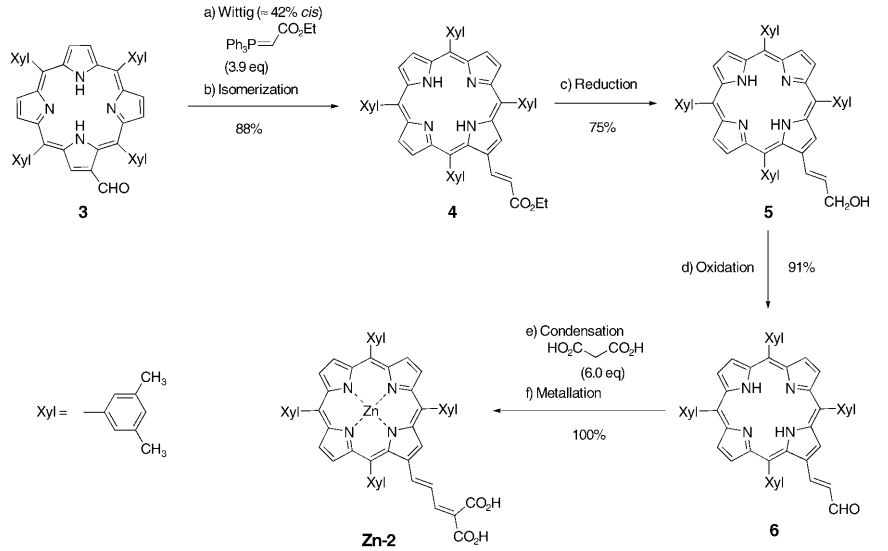

Scheme 1. Reagents and conditions: a) Toluene, reflux (≈24 h), N_2. b) *i*: I_2 (1.0 eq), $CHCl_3$, RT (≈17 h); *ii*: Saturated $Na_2S_2O_3$ (excess). c) *i*: DIBAL-H (3.0 eq), toluene, 0 °C (30 min)→RT (30 min)→0 °C, argon; *ii*: MeOH. d) MnO_2 (excess), CH_2Cl_2, RT (≈26 h) reflux (1.5 h). e) $NH_4^+AcO^-$ (6.0 eq), AcOH, 70 °C (3 h), N_2). f) $Zn(OAc)\cdot 2H_2O$ (4.0 eq), 70 °C (15 min).

Table 1. Electronic absorption and emission data for zinc porphyrins.

Complex	Absorption[a] λ_{max} [nm] (ε [10^{-3} M^{-1}cm^{-1}])	Emission[b]		Electrochemical data [eV][c]	
		λ_{max} [nm]	τ [ns]	HOMO	LUMO
Zn-1	sh 429 (92.4), 455 (153) 571 (12.7) 620 (11.9)	670	4	−5.62	−3.36
Zn-2	326 (24.0), sh 431 (116) 443 (120), 570 (15.9) 618 (12.5)	670	3	−5.52	−3.56

[a] Absorption data were obtained in THF solution at 298 K. [b] Emission spectra were obtained for argon-degassed solutions in THF, at 298 K, by excitation at 570 nm. [c] The electrochemical data were measured in DMF with 0.1 M $TBAPF_6$ as supporting electrolyte using a gold (or glassy carbon) electrode.

The electronic absorption, emission, and electrochemical data for **Zn-1** and **Zn-2** are given in Table 1. Figure 2 shows the absorption and emission spectra of **Zn-1** measured in THF solution at room temperature. The metalloporphyrins show a series of absorption bands (between 400 and 650 nm) due to π–π* transitions of the conjugated macrocycle. Both compounds show red-shifts in the Soret and Q bands with respect to zinc tetraphenylporphyrin (ZnTPP) and increased molar extinction coefficients for the Q bands due to the extended conjugation and the electron-withdrawing nature of the anchoring groups.[17] The red-shift of the Q bands in **Zn-1** compared to **Zn-2** is due to the stronger electron-withdrawing nature of the

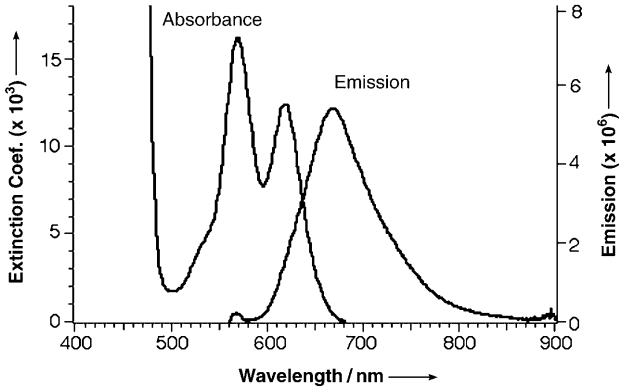

Figure 2. Absorption and emission spectra of porphyrin **Zn-1** in THF.

cyanide group. The visible absorption spectra of both **Zn-1** and **Zn-2**, adsorbed on a TiO_2 film, show features similar to those seen in the corresponding solution spectra, but exhibit a small red-shift due to the interaction of the anchoring groups with the surface.[20] The emission data of metalloporphyrins **Zn-1** and **Zn-2** were obtained at room temperature by excitation at 570 nm in THF solution; the spectra show characteristic maxima at 670 nm.[17] The emission time constants are several orders of magnitude greater than the electron-injection rate into the conduction band of TiO_2.

Figure 3 shows the energy-level diagram for **Zn-1** obtained from cyclic voltammetry measurements in dimethylformamide (DMF) using 0.1 M tetrabutylammonium hexafluorophosphate

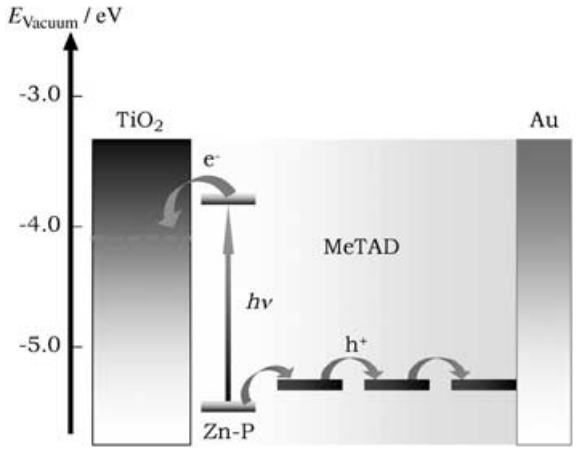

Figure 3. Charge-separation process occurring in a Zn-Porphyrin-sensitized heterojunction and approximate vacuum energy levels. The energy levels portrayed are for **Zn-1**.

($TBAPF_6$) as supporting electrolyte. The HOMO and LUMO of **Zn-1** are at −5.62 and −3.46 eV, respectively; for **Zn-2** they are at −5.52 and −3.56 eV, respectively. The HOMOs of both **Zn-1** and **Zn-2** are slightly more negative than that of the standard dye *cis*-dithiocyanatobis(4,4′-dicarboxylic acid-2,2′-bipyridine) ruthenium(II), which makes the regeneration of the porphyrin dyes more favorable. In addition, cyclic voltammetric measurements on porphyrin monolayers adsorbed on TiO_2[17] indicate that—probably as a result of the highly delocalized structure of the porphyrins and an effective overlap of neighboring molecules—lateral charge hopping takes place within the monolayer itself.[21] This process alleviates the problem of the lack of intimate contact between the adsorbed dye and the hole conductor, since the dye can be regenerated through lateral hole hopping between dye molecules.

Mesoporous solid-state heterojunction cells, incorporating **Zn-1** and **Zn-2**, were prepared as previously described.[12] A photograph of one of the bright-green-colored fabricated solar cells is shown in Figure 4, and the photocurrent action spectra

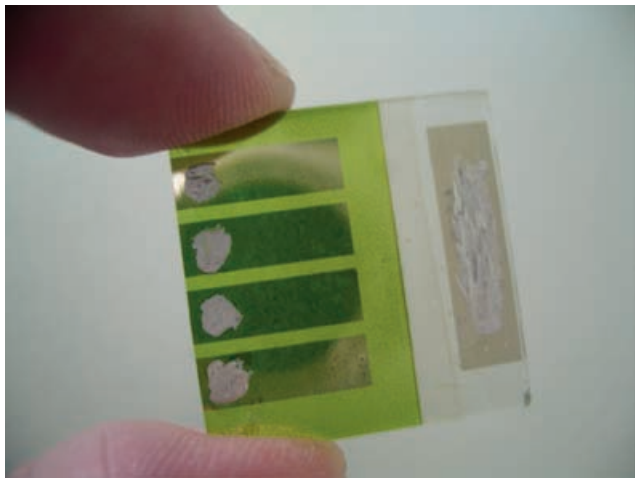

Figure 4. A photograph of the fabricated solid-state **Zn-1** sensitized heterojunction solar cells.

obtained from the **Zn-1** and **Zn-2** sensitized heterojunction devices is given in Figure 5. The shapes of the action spectra are similar to those of the corresponding absorption spectra. For **Zn-1**, the incident monochromatic photon-to-current conver-

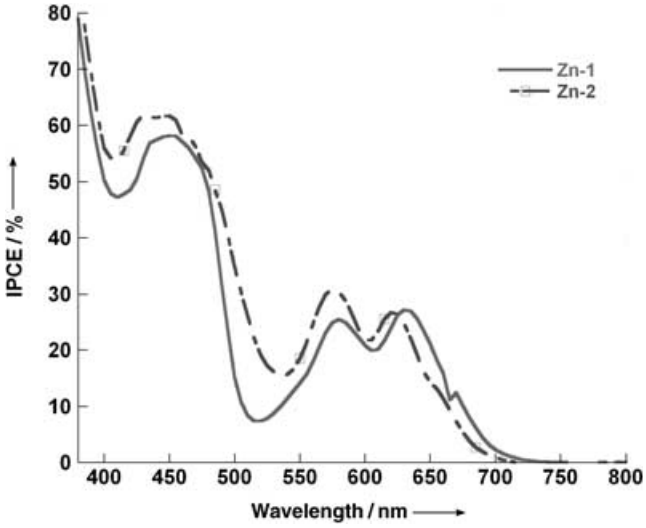

Figure 5. Photocurrent action spectra obtained for the **Zn-1** and **Zn-2** sensitized heterojunction devices.

sion-efficiency (IPCE) values peak at about 65% in the Soret-band region, but in the Q-band region, the highest value is only 25%. In the corresponding dye-sensitized liquid-junction cell, however, the IPCE peaks are at 90% in the Soret-band region and 70% in the Q-band region. It should also be noted that the IPCE values in **Zn-2** porphyrin-sensitized heterojunctions are substantially better than that previously obtained for the analogous ruthenium-dye-sensitized heterojunction.[13]

Figure 6 show the current and voltage characteristics of the **Zn-1** and **Zn-2** sensitized heterojunction cells under simulated

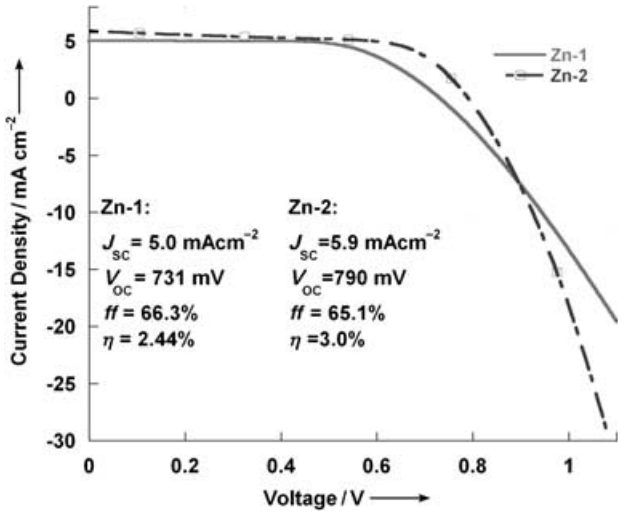

Figure 6. Photocurrent–voltage characteristics of the nanocrystalline photoelectrochemical cell, sensitized with **Zn-1** and **Zn-2**, in THF under simulated global AM 1.5 solar radiation.

global AM 1.5 light intensity (1000 W m^{-2}). For the **Zn-2** sensitized cell, the short-circuit photocurrent density (J_{sc}) of 5.9 mA cm^{-2}, open-circuit photovoltage (V_{oc}) of 790 mV, and fill factor (*ff*) of 0.65 yield an overall conversion efficiency η, derived from the equation: $\eta = J_{sc} \times V_{oc} \times ff$, of 3%. The corresponding values for the **Zn-1** sensitized cell are 5.1 mA cm^{-2}, 730 mV, 0.66, and 2.5%. In spite of this, there is still a need to further improve the cell performances, since the efficiencies of the solid-state devices are only about half of those obtained in liquid-junction cells.[17] Nevertheless, the porphyrin-sensitized cells demonstrate greatly improved efficiencies, and the porphyrin molecules themselves are readily functionalized. Attempts to further improve the solid-state cells will concentrate on improving the overall IPCE performance by tuning both the porphyrin sensitizers and the structure of the hole conductors.

Our findings open up new avenues for the design and development of new sensitizers that show directionality in their excited states and near-IR responses. The nanocrystalline TiO_2 photovoltaic cell containing these sensitizers would remain translucent to the eye, while absorbing enough solar photons in the near-IR region to render efficiencies acceptable for practical applications, such as photovoltaic windows.

Experimental Section

General: ^{1}H NMR spectra were obtained at 400.13 MHz using a Brucker 400 spectrometer and an X-WIN NMR software. The chemical shifts are relative either to tetramethylsilane (TMS) or to the residual proton signal in deuterated solvents ($CDCl_3$ δ 7.27). ^{13}C NMR shifts are relative to $CDCl_3$ (δ 77.0) or CD_2Cl_2 (δ 53.1). Chemical shifts are reported as position (δ), multiplicity (s = singlet, d = doublet, t = triplet, q = quartet, dd = doublet of doublets, m = multiplet), relative integral, coupling constant (*J* in Hz), and assignment. Full structural assignments were assisted by the acquisition of appropriate data from 2D experiments (COSY, HMQC, HMBC).

UV/Vis/NIR spectra were collected on a Shimadzu UV-3101PC UV/Vis/NIR scanning spectrophotometer controlled by a Shimadzu software. AR-, HPLC-, or spectroscopy-grade solvents were used in all cases.

High-resolution mass spectrometry (HRMS) (fast-atom bombardment, FAB, and electron ionization, EI) was carried out using a Varian VG70–250S double-focusing magnetic-sector mass spectrometer. Samples analyzed by FAB-HRMS were supported on an *m*-nitrobenzyl alcohol matrix (unless otherwise stated). The data were put through a MASSPEC II data system to give $\pm$5 ppm error formulations on molecular ions. Major fragmentations are given as percentages relative to the base-peak intensity.

Melting-point determinations were performed on a Cambridge Instruments Kofler hot stage and were not corrected.

Column chromatography was performed using Merck Kieselgel 60 (230–400 mesh) and thin-layer chromatography was carried out using precoated silica-gel plates (Merck Kieselgel $^{60}F_{254}$).

The reagents and solvents used herein came from many different sources and were generally AR-grade reagents. Chromatography solvents were laboratory grade and were distilled before use. For most applications, water was treated with a reverse-osmosis filtration system. Higher purity water was obtained by distilling Milli-Q H_2O off activated charcoal. Dry degassed CH_2Cl_2 and DMF were prepared by distillation of the AR-grade solvent over CaH_2 under an N_2 atmosphere. Dry toluene, ether, benzene, and THF were prepared by passing the argon-degassed solvent through activated alumina columns. N_2 (oxygen-free) was passed through a KOH drying column to remove moisture.

Construction of Heterojunction Cells: Mesoporous solid-state heterojunction cells were prepared as previously described.[12] A smooth TiO_2 film (with thickness $<$ 100 nm) was deposited by spray pyrolysis onto a transparent-conducting-oxide (TCO) glass (F-doped SnO_2 coating, sheet resistance: 10 Ohm square^{-1}, 80% transmission in the visible range, obtained from Asahi TCO Glass). This compact film serves to avoid short-circuiting of the two current collectors by the hole conductor. A nanocrystalline TiO_2 film ($\approx$2 μm thick) was deposited onto the first layer by doctor blading and subsequent annealing at 450 °C of a paste containing 18-nm-sized anatase particles. A monolayer of the sensitizer was adsorbed onto this film by dipping it into a 2×10^{-4} M solution of the sensitizer dissolved in THF and leaving it there overnight. A concentrated (0.17 M) solution of spiro-MeOTAD in chlorobenzene was spin-coated onto the dye-loaded film, and the solvent was removed by evaporation in vacuum. The hole-conductor solution was doped with tris(4-bromophenyl)ammoniumylhexachloroantimonate (0.3 mM) and contained 13 mM of lithium triflate, as well as 0.13 M of *tert*-butylpyridine, as additives to increase the conductivity of the hole-conducting layer and the potential of the cell. A 30-nm-thick layer

of gold was applied by evaporation in vacuum to serve as an ohmic back contact.

Synthesis: **4**: 3-*trans*-(5′,10′,15′,20′-tetrakis(3′′,5′′-dimethylphenyl)-porphyrin-2′-yl)acrylic acid ethyl ester: Wittig: A solution of porphyrin aldehyde **3**[18] (400 mg, 0.530 mmol) and ethyl (triphenylphosphoranylidene)acetate (730 mg, 2.07 mmol, 3.9 eq) in dry toluene (37 mL) was heated at reflux temperature under N_2. After 19.5 h, TLC analysis (silica, toluene) indicated that all of the starting material **3** had been consumed. After cooling to room temperature (RT), the solvent was removed in vacuo. The residue was column-chromatographed [silica, 45 $mm_{dia}\times$120 mm, 2:1→1:0(CH_2Cl_2:hexane)] collecting the major purple-colored fraction to give a *cis*/*trans* isomeric mixture of the porphyrin ethyl ester **4** (351 mg, ≈42% *cis* by ^{1}H NMR, 80%) as a purple solid. ^{1}H NMR (270 MHz, $CDCl_3$, TMS, selected data only): δ−2.740 (s, NH_{cis}), −2.641 (s, NH_{trans}), 0.891 (t, ^3J=7.1 Hz, CH_2–C**H**$_{3\text{-}cis}$), 4.013 (q, ^3J=7.1 Hz, C**H**$_2$–$CH_{3\text{-}cis}$), 5.658 (d, ^3J=12.1 Hz, $H_{cis\text{-ethenyl}}$), 6.866 (dd, ^3J=12.1 Hz, ^4J=1.3 Hz, $H_{cis\text{-ethenyl}}$).

Isomerization: The isomeric mixture was dissolved in $CHCl_3$ (20 mL), and I_2 (108 mg, 0.426 mmol, 1.0 eq) was added. After stirring at RT for 17 h in the dark, excess saturated $Na_2S_2O_3$ (≈20 mL) was added; stirring continued for further 15 min. The organic layer was separated and dried (K_2CO_3), and the product was precipitated with methanol to give *trans* **4** (339 mg, 97%, 78% overall) as a dark-brown powder. ^{1}H NMR (400 MHz, $CDCl_3$, TMS): δ −2.642 (br s, 2H, NH), 1.387 (t, 3H, ^3J=7.2 Hz, OCH_2–C**H**$_3$), 2.57–2.61 (m, 24H, $H_{Me\text{-}Xyl}$), 4.254 (q, 2H, ^3J=7.1 Hz, OC**H**$_2$–CH_3), 6.574 (d, 1H, ^3J=15.6 Hz, H_2), 7.38–7.44 (m, 5H, 1H_3+4$H_{p\text{-}Ph}$), 7.743 (br s, 2H, $H_{o\text{-}Ph}$), 7.80–7.82 (m, 6H, $H_{o\text{-}Ph}$), 8.81–8.86 (m, 6H, $H_{pyrrolic}$), 8.972 (br s, 1H, $H_{3'\,pyrrolic}$).

The assignments are aided by COSY spectra. UV/Vis (CH_2Cl_2): λ_{max} (nm) (ε [10^{-3} м$^{-1}$cm^{-1}]) 431 (283), 524 (19.0), 563 (8.32), 602 (6.30), 659 (4.15). FAB-LRMS: *m/z* (%, assignment) cluster at 823–827, 825 (100, MH^+). HRMS: Calcd. for MH^+ ($C_{57}H_{52}N_4O_2$): 825.4169, found: 825.4178.

5: 3-*trans*-(5′,10′,15′,20′-tetrakis(3′′,5′′-dimethylphenyl)porphyrin-2′-yl)allyl hydroxide: DIBAL-H (2.30 mL, 1.5 м in toluene, 3.45 mmol, 3.0 eq) was added to a solution of porphyrin ester **4** (954 mg, 1.16 mmol) in dry toluene (30 mL) under an argon atmosphere at 0 °C. After 30 min, the solution was allowed to warm to RT. After further 30 min, the solution was cooled to 0 °C and MeOH (5.0 mL) was added, followed by the addition of aqueous potassium sodium L-tartrate tetrahydrate (5 g in 150 mL). EtOAc (150 mL) was added, and the organic layer was washed with saturated aqueous $NaHCO_3$ and dried ($MgSO_4$). The solvent was then removed in vacuo. The residue was column-chromatographed [silica, 45 $mm_{dia}\times$160 mm, CH_2Cl_2:Et_2O (98:2)] collecting the major red-colored fraction. The product was precipitated with hexane to give **5** (675 mg, 75%) as a purple powder. ^{1}H NMR (400 MHz, $CDCl_3$, TMS): δ −2.732 (br s, 2H, NH), 2.56–2.61 (m, 24H, $H_{Me\text{-}Xyl}$), 4.169 (t, 2H, ^3J=5.4 Hz, C**H**$_2$OH), 6.313 (dd, 1H, ^3J=15.6 Hz, ^4J=0.8 Hz, $H_{3\,ethenyl}$), 6.514 (dt, 1H, ^3J=15.6 Hz, ^3J=5.4 Hz, $H_{2\,ethenyl}$), 7.38–7.45 (m, 4H, $H_{p\text{-}Xyl}$), 7.72 (br s, 2H, $H_{o\text{-}Xyl}$), 7.81–7.83 (br s, 6H, $H_{o\text{-}Xyl}$), 8.79–8.85 (m, 7H, $H_{pyrrolic}$).

The Assignments are aided by COSY spectra: UV/Vis (CH_2Cl_2): λ_{max} (nm) (ε [10^{-3} м$^{-1}$cm^{-1}]) 424 (322), 520 (18.1), 557 (7.29), 595 (5.75), 653 (3.78). FAB-LRMS: *m/z* (%, assignment) cluster at 781–786, 783 (100, MH^+). HRMS: Calcd. for MH^+ ($C_{55}H_{50}N_4O_1$): 783.4063, found: 783.4077.

6: 3-*trans*-(5′,10′,15′,20′-tetra(3′′,5′′-dimethylphenyl)porphyrin-2′-yl)-allylaldehyde: Activated MnO_2 (1.82 g, 20.9 mmol) was added to a solution of allyl hydroxide **5** (665 mg, 850 moμl) in dry CH_2Cl_2 (13.0 mL) and stirred at RT for 26 h. After heating to reflux temperature for 1.5 h under N_2 atmosphere, TLC analysis (silica, CH_2Cl_2, R_f=0.5) indicated that all the staring material had been consumed, with the appearance of a single new (less-polar) band. On cooling to room temperature, the solution was filtered through celite, and the solvent was removed in vacuo. Precipitation with methanol gave **6** (606 mg, 91%) as a purple crystalline solid. ^{1}H NMR (400 MHz, $CDCl_3$, TMS): δ −2.602 (br s, 2H, NH), 2.570 (s, 6H, $H_{Me\text{-}Xyl}$), 2.601 (s, 12H, $H_{Me\text{-}Xyl}$), 2.612 (s, 6H, $H_{Me\text{-}Xyl}$), 6.914 (dd, 1H, ^3J=15.5 Hz, ^3J=7.9 Hz, $H_{2\,ethenyl}$), 7.053 (d, 1H, ^3J=15.4 Hz, $H_{3\,ethenyl}$), 7.407 (s, 2H, $H_{p\text{-}Xyl}$), 7.435 (s, 1H, $H_{p\text{-}Xyl}$), 7.471 (s, 1H, $H_{p\text{-}Xyl}$), 7.77 (br s, 2H, $H_{o\text{-}Xyl}$), 7.80–7.83 (m, 6H, $H_{o\text{-}Xyl}$), 8.79–8.93 (m, 6H, $H_{pyrrolic}$), 9.021 (s, 1H, $H_{pyrrolic}$), 9.270 (d, 1H, ^3J=7.9 Hz, C**H**O).
The assignments are aided by COSY spectra. UV/Vis (CH_2Cl_2): λ_{max} (nm) (ε [10^{-3} м$^{-1}$cm^{-1}]) 437 (225), 527 (18.0), 569 (7.52), 606 (6.08), 663 (5.47). FAB-LRMS: *m/z* (%, assignment) cluster at 779–784, 781 (100, MH^+). HRMS: Calcd. for MH^+ ($C_{55}H_{48}N_4O_1$): 781.3906, found: 781.3901.

Zn-2: 2-Carboxy-5-(2′-(5′,10′,15′,20′-tetrakis(3′′,5′′-dimethylphenyl)-porphyrinato zinc-(II))yl)penta-2,4-dienoic acid: A solution of **6** (200 mg, 256 moμl), malonic acid (160 mg, 1.54 mmol, 6.0 eq), and ammonium acetate (118 mg, 1.53 mmol, 6.0 eq) in a solution of acetic acid (5.0 mL) was heated at 70 °C for 3 h. $Zn(OAc)_2{\cdot}2H_2O$ (222 mg, 1.01 mmol, 4.0 eq) was added to the resulting red solution and heated at 70 °C for 15 min. On cooling to room temperature, sufficient H_2O was added, precipitating the product to give **Zn-2** (238 mg, 100%) as a purple solid. ^{1}H NMR (400 MHz, [D_6]DMSO, TMS): δ 2.544 (s, 6H, $H_{Me\text{-}Xyl}$), 2.577 (s, 12H, $H_{Me\text{-}Xyl}$), 2.601(s, 6H, $H_{Me\text{-}Xyl}$), 6.514 (d, 1H, ^3J=15.1 Hz, $H_{5\,pentadienyl}$), 7.163 (d, 1H, ^3J=11.6 Hz, $H_{3\,pentadienyl}$), 7.423 (s, 2H, $H_{p\text{-}Xyl}$), 7.459 (s, 1H, $H_{p\text{-}Xyl}$), 7.513 (s, 1H, $H_{p\text{-}Xyl}$), 7.691 (s, 2H, $H_{o\text{-}Xyl}$), 7.77–7.81 (m, 7H, 6$H_{o\text{-}Xyl}$+1$H_{4\,pentadienyl}$), 8.74–8.80 (m, 6H, $H_{pyrrolic}$), 8.911 (br s, 1H, $H_{3'\,pyrrolic}$).
The assignments are aided by COSY and LR-COSY spectra. UV/Vis (THF): λ_{max} (nm) (ε [10^{-3} м$^{-1}$cm^{-1}]) 326 (24.0), sh 431 (116), 443 (120), 570 (15.9), 618 (12.5). FAB-LRMS: *m/z* (%, assignment) cluster at 928–934, 928 (100, MH^+). HRMS: Calcd. for M^+ ($C_{58}H_{48}N_4O_4Zn$): 928.2967, found: 928.2966.

Acknowledgements

This work was supported by the Swiss Federal Office for Energy (OFEN) and U. S. Air Force Research Office under contract number F61775–00-C0003, and the New Zealand Foundation for Research, Science and Technology New Economy Research Fund contracts MAUX0014 and MAUX0202. LSM thanks the German Research Foundation (DFG) for funding (Emmy-Noether Stipendium). We thank P. Comte for his kind assistance in obtaining TiO_2 electrodes.

Keywords: photovoltaic cells · porphyrins · sensitizers · solar cells · thin films

[1] B. O'Regan, M. Grätzel, *Nature* **1991**, *353*, 737.
[2] M. Grätzel, *Nature* **2001**, *414*, 338.
[3] M. K. Nazeeruddin, A. Kay, I. Rodicio, R. Humphry-Baker, E. Muller, P. Liska, N. Vlachopoulos, M. Grätzel, *J. Am. Chem. Soc.* **1993**, *115*, 6382.
[4] U. Bach, D. Lupo, P. Comte, J.-E. Moser, F. Weissörtel, J. Salbeck, H. Spreitzer, M. Grätzel, *Nature* **1998**, *395*, 583.
[5] J. Krüger, R. Plass, M. Grätzel, H. Matthieu, *J. App. Phys. Lett.* **2002**, *81*, 367.

[6] P. Wang, S. M. Zakeeruddin, J. Moser, M. K. Nazeeruddin, T. Sekiguchi, M. Graetzel, *Nat. Mater.* **2003**, *2*, 402.
[7] M. Grätzel, J. -E. Moser in *Molecular-Level Electronics, Imaging and Information, Vol. 5: Solar Energy Conversion* (Eds.: V. Balzani, I. Gould), Wiley-VCH, Weinheim, **2001**, pp. 589 – 644.
[8] M. Gra1tzel, *J. Photochem. Photobiol., C* **2003**, *4*, 145.
[9] P. Wang, Q. Dai, S. M. Zakeeruddin, M. Forsyth, D. R. MacFarlane, M. Grätzel, *J. Am. Chem. Soc.* **2004**, *126*, 13590.
[10] W. Kubo, K. Murakoshi, T. Kitamura, S. Yoshida, M. Haruki, K. Hanabusa, H. Shirai, Y. Wada, S. Yanagida, *J. Phys. Chem. B* **2001**, *105*, 12809.
[11] B. O'Regan, F. Lenzmann, R. Muis, J. Wienke, *Chem. of Materials* **2002**, *14*, 5023.
[12] U. Bach, D. Lupo, P. Compte, J. E. Moser, F. Weissörtel, J. Salbeck, H. Spreitzer, M. Grätzel, *Nature* **1998**, *395*, 583.
[13] J. Kruger, R. Plass, L. Cevey, M. Piccirelli, M. Gra1tzel, *Appl. Phys. Lett.* **2001**, *79*, 2085.
[14] Y. Tachibana, S. A. Haque, I. P. Mercer, J. R. Durrant, D. R. Klug, *J. Phys. Chem. B* **2000**, *104*, 1198.
[15] S. Cherian, C. C. Wamser, *J. Phys. Chem. B* **2000**, *104*, 3624.
[16] W. M. Campbell, A. K. Burrell, D. L. Officer, K. W. Jolley, *Coord. Chem. Rev.* **2004**, *248*, 1363.
[17] Q. Wang, W. M. Campbell, K. W. Jolley, D. L. Officer, P. J. Walsh, K. Gordon, R. Humphry-Baker, M. K. Nazeeruddin, M. Graetzel, unpublished results.
[18] W. J. Belcher, A. K. Burrell, W. M. Campbell, D. L. Officer, D. C. W. Reid, K. Y. Wild, *Tetrahedron* **1999**, *55*, 2401.
[19] W. M. Campbell, D. L. Officer, M. K. Nazeeruddin, M. Graetzel, unpublished results.
[20] M. K. Nazeeruddin, R. Humphry-Baker, P. Liska, M. Grätzel, *J. Phys. Chem. B* **2003**, *107*, 8981.
[21] P. Papageorgiou, M. Graetzel, *J. Phys. Chem. B* **2002**, *106*, 3813.